The effect of annealing on the properties of $CdS_{0.95}Se_{0.05}$ nanoparticles dispersed in oxide glass containing Zn

1997 J. Phys.: Condens. Matter 9 9745

(http://iopscience.iop.org/0953-8984/9/45/005)

J. Phys.: Condens. Matter **9** (1997) 9745–9757. Printed in the UK PII: S0953-8984(97)86904-4

The effect of annealing on the properties of $CdS_{0.95}Se_{0.05}$ nanoparticles dispersed in oxide glass containing Zn

M Rajalakshmi, T Sakuntala† and Akhilesh K Arora

Materials Science Division, Indira Gandhi Centre for Atomic Research, Kalpakkam, TN 603102, India

Received 13 August 1997

Abstract. The optical and vibrational properties of $CdS_{0.95}Se_{0.05}$ nanoparticles dispersed in oxide glass containing Zn are investigated as functions of the annealing temperature using photoluminescence, optical absorption and Raman spectroscopy. Upon annealing the samples, a blue-shift of the optical absorption and photoluminescence is observed, in contrast to the expected red-shift due to particle growth. This can be understood if one invokes the inclusion of Zn into the particle which more than compensates the red-shift due to particle growth. The observed increase in the LO phonon frequency upon annealing also confirms this. The particle size, obtained from the analysis of low-frequency Raman spectra in terms of confined acoustic phonons, shows considerable growth upon annealing above 550 °C. Overtones up to 3-LO are identified. Furthermore, the LO phonon and its overtones are found to exhibit strong resonance enhancement as a function of exciting wavelength. However, upon annealing, the Raman intensities reduce dramatically due to the shift of the electronic transition energy away from that of the incident photon.

1. Introduction

Electronic, optical and vibrational properties of small semiconductor particles such as those of II–VI compounds differ considerably from those of bulk crystals, when their sizes are in the region of a few nanometres [1, 2]. The departures of these properties from the bulk values are measurable only when the particle size is typically 20 times the lattice parameter or less. The changes in the electronic structure and consequently in the optical properties arise from the confinement of the electron wavefunction in a small region of space and the electronic energy levels of such a system are analogous to those of a particle in a box [3, 4]. This results in an increase in the direct interband transition energy; the dominant term of this increase is proportional to d^{-2} where d is the diameter of the particle [3]. This dependence on size has been exploited in tailoring the properties of long-pass optical filters. In addition, these semiconductor nanoparticle systems (also known as quantum dots) dispersed in a suitable optically transparent host, have exhibited excellent nonlinear optical properties [5, 6], saturable absorption [7] and optical bistability [8]. An increase in the efficiency of the radiative recombination by several orders of magnitude has also been reported for quantum dots of indirect-gap semiconductors [9, 10]. Similarly, confinement of phonons within the particle also leads to interesting changes in the vibrational spectrum [11]. Confined acoustic phonons become observable in the low-frequency Raman spectra [12, 13]. Optical phonon lineshapes develop marked asymmetry [14] and surface optical

† Present address: Solid State Physics Division, Bhabha Atomic Research Centre, Mumbai 400 085, India.

0953-8984/97/459745+13$19.50

phonons are also observed [15]. The motivation of basic studies of such systems has been that of developing an understanding of the electronic, optical and vibrational properties of new materials so that their properties can be tailored for optical, electro-optical and nonlinear optical applications.

Semiconductor quantum dot systems are conventionally synthesized either by colloidal precipitation [16, 17] or in oxide glass hosts [14, 18]. Recently, synthesis of CdS quantum dots in polymer films has also been reported [19]. In the case of semiconductor-doped oxide glasses, annealing of the glass obtained after quenching the melt leads to the precipitation of the semiconductor from the solid solution. The annealing temperature and time determine the size of the semiconductor nanoparticles [20]. Borosilicate glasses containing particles of $CdS_{1-x}Se_x$ mixed crystals have been most extensively investigated. Various models and regimes of nucleation, growth and ripening have been examined for these systems [21]. The size distribution during the early stages is found to be in accordance with the homogeneous nucleation theory [22]. A diffusion-limited growth and subsequent ripening has been concluded from the analysis of optical absorption [23]. The ripening stage was found to follow the Lifshitz–Slyozov law [24]. Most of these studies on growth kinetics have been carried out using transmission electron microscopy and optical absorption spectroscopy. The results have been reported only for the '*early stage*' of nucleation and growth [25] while the '*late stage*' of particle growth has not been studied in detail. There have also been attempts to estimate the particle size from the analysis of optical absorption data alone. This involves several parameters such as size distribution, effective mass, and the oscillator strength of different interband transitions, the values of which had to be set rather arbitrarily [25]. Furthermore, the behaviour of optical properties of the $CdS_{1-x}Se_x$ system in glasses containing Zn appears to be different [20, 26] from that of those without Zn [24, 27]. The presence of Zn in the glass host appears to influence the composition of the particle, i.e. some amount of Zn also gets incorporated in the particle. Sukumar and Doremus [26] reported the evolution of the optical absorption edge of CdS-doped borosilicate glass containing zinc, but the zinc content of the particles was not analysed. The blue-shift of the optical absorption edge was explained as arising from the quantum-size effect; however, the consequences of changes in the particle stoichiometry were not considered. Borrelli *et al* [20] reported incorporation of Zn into the CdS particles during prolonged annealing at elevated temperatures from the analysis of x-ray data using Vegard's law. The changes in the optical absorption data were assigned to the change in the stoichiometry of the particle of $Zn_yCd_{1-y}S$. These results strongly suggest that the optical properties are strongly influenced by *competing* effects arising from the particle size growth as well as changes in the stoichiometry of the particle. This aspect has not been studied in detail. Furthermore, as mentioned earlier, analysis of results from just one technique is often not sufficient to characterize the system. On the other hand, use of several complementary techniques would yield more complete information and understanding of the system.

In the present work we report an optical absorption, Raman spectroscopic and photoluminescence study of semiconductor-doped glass (Schott GG475) after various annealing treatments. Low-frequency Raman spectra are analysed to estimate the particle size. The effect of annealing on the optical absorption, photoluminescence (PL) energy, and the frequencies of the longitudinal optic (LO) phonon and its overtones are discussed in the context of possible changes in the size and composition of the particle. Resonance effects on the Raman intensities are also reported. The present studies represent the '*late stage*' of annealing which has not been well studied previously.

2. Experimental details

Raman and photoluminescence spectra of the untreated and annealed samples were recorded in the back-scattering geometry at room temperature. The sample used in the present study is semiconductor-doped oxide glass (optical filter GG475) obtained from Schott Glaswerke, Germany. The typical composition of the host glass by weight is SiO_2 (≈50%), K_2O (≈20%), ZnO (≈20%), B_2O_3 (≈8%). The remaining 2% is constituted by the dopant semiconductors CdS and CdSe [28]. The selenium content in the sample was estimated to be 5% of the total chalcogen amount from the inductively coupled plasma mass spectroscopy (ICPMS). The samples were annealed at different temperatures between 500 and 700 °C for 5 h. The annealing temperatures are controlled accurate to ±1 °C using a proportional temperature controller. Raman scattering, PL and optical absorption measurements of the untreated and annealed samples were carried out at room temperature. The 406.7 nm line of a krypton-ion laser and the 454.5, 457.9, 465.8, 472.7, 476.5, 488.0, 496.5, 501.7, and 514.5 nm lines of an argon-ion laser were used to excite the photoluminescence and Raman spectra. Scattered light from the sample was analysed using a Spex double monochromator and detected using a cooled photomultiplier tube operated in the photon-counting mode. Scanning of the spectra and data acquisition were carried out using a home-built microprocessor-based data-acquisition-cum-control system. Subsequent to the completion of a scan, data were transferred to a personal computer for further analysis. The optical absorption spectra were recorded using a Chemita 2500 UV-VIS Spectrophotometer.

3. Results and discussion

As mentioned in the introduction, the presence of zinc in the base glass can influence the optical properties of the $CdS_{1-x}Se_x$ nanoparticles [20, 25]. In order to understand the behaviour of the phonon spectrum and optical properties as functions of the particle size, one must also estimate the stoichiometry and the size of the particles. In the present investigation the composition of the particles is estimated from the LO phonon frequency. The particle size is obtained from the frequency of the confined acoustic phonons (spheroidal modes) observed in the low-frequency Raman (LFR) spectra. We first present the results of photoluminescence and optical absorption studies.

3.1. Photoluminescence and optical absorption

Photoluminescence and optical absorption in the particle arises from the direct electronic transitions between the valence and conduction band which are modified as compared to those in the bulk, due to the confinement of the electron and hole within the particle. The energy of the lowest excited state is [3]

$$E(d) = E_b + \frac{2\bar{h}^2\pi^2}{d^2}\frac{1}{\mu} \tag{1}$$

where E_b is the bulk band gap and μ is the reduced mass. The second term is the most dominant size-dependent term and it represents the energy of quantum localization. As a consequence of carrier confinement, the optical absorption edge and PL peak appear at higher energy. It may be noted from equation (1) that the PL energy and the absorption edge are expected to show red-shifts [20, 27] as the particle size increases. PL spectra of untreated samples and those annealed at various temperatures between 500 and 700 °C were recorded using the 406.7 nm line of a krypton laser. Figure 1 shows the PL spectra of

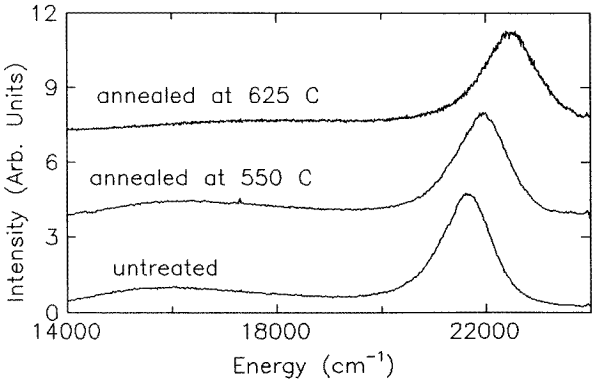

Figure 1. Photoluminescence spectra of untreated semiconductor nanoparticles and after annealing at 550 and 625 °C. The spectra are excited using the 406.7 nm line of a krypton-ion laser. The spectrum corresponding to 625 °C is magnified by a factor of two for the sake of clarity.

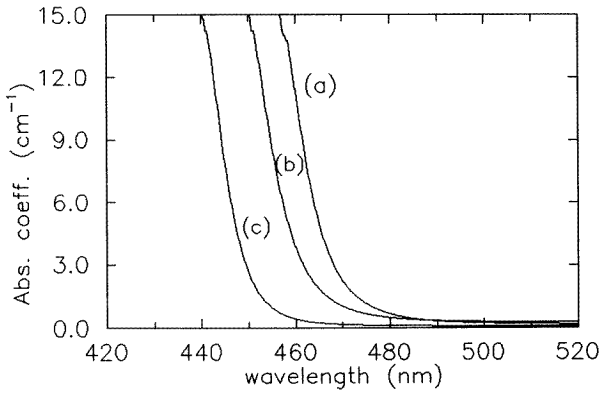

Figure 2. Optical absorption spectra of an untreated sample (a) and the sample after annealing at 550 (b) and 625 °C (c). Note the shift of the onset of absorption upon annealing to shorter wavelengths (higher energies).

samples annealed at 550 and 625 °C along with that of an untreated sample. Note the shift of the PL peak to higher energies due to annealing, in contrast to the behaviour expected due to the growth of the particles [27]. The optical absorption spectra of samples after different annealing treatments are shown in figure 2. Note that the onset of optical absorption also shifts to higher energies upon annealing. This behaviour is similar to that of the PL energy found in the present studies. Figure 3 shows the dependence of the PL energy and the onset of the optical absorption on the annealing temperature.

Before we proceed to analyse the blue-shifts observed in the PL and optical absorption upon annealing, it is worth comparing the present results with those reported for very similar Schott glass [29]. It may be mentioned that the semiconductor-doped glasses studied in [29] were as-quenched samples (precursors of the filter GG495) with negligibly small absorption. This is because, to start with, the semiconductor is homogeneously distributed in the glass and measurable absorption results only after the semiconductor nanoparticles have grown

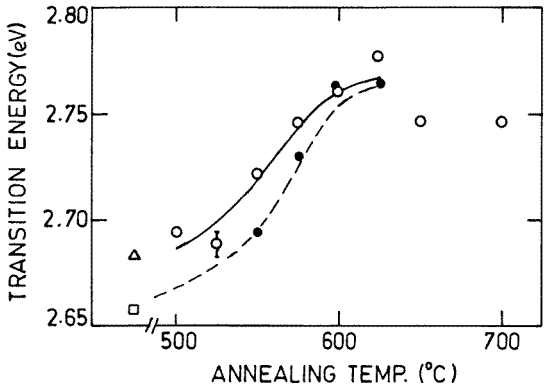

Figure 3. The energy of the PL peak (○) and that of the onset of absorption (●) as functions of the annealing temperature. The solid and dashed curves are guides to the eye. The symbols △ and □ correspond to the energy of the PL and that of the onset of optical absorption, respectively, for the untreated sample.

considerably due to annealing. The optical absorption under such conditions exhibits a blue-shift with respect to the bulk band gap, due to the carrier confinement effect. The amount of blue-shift is found to reduce upon further annealing due to particle size growth. Similarly, in another recent optical absorption study of the growth of $Cd_{1-y}Zn_yS$ particles, only a reduction in blue-shift is observed as a function of annealing temperature [25]. On the other hand the untreated samples used in the present study are actually samples of the filter GG475 which have already undergone some heat treatment at Schott Glaswerke. Thus the present heat treatments correspond to the 'late stages' of annealing while those reported earlier [25, 29] represent the 'early stage'.

The blue-shift observed in the present annealing treatment has not been reported earlier. Such a blue-shift can arise if during annealing some amount of Zn replaces Cd in the particle. The band gap in the $Cd_{1-y}Zn_yS$ system is known to increase with increasing y. Hence a blue-shift can arise if the increase in the band gap arising from the change in stoichiometry more than compensates the red-shift expected from the particle size growth. However, in order to confirm this one must estimate the composition as well as the size of the particle after each heat treatment. This analysis is carried out in the following sections. The composition is estimated from the analysis of LO phonon frequencies, whereas the particle size is obtained from that of the low-frequency Raman spectra.

3.2. Longitudinal optical phonons

Confined optical phonons were first discovered in semiconductor superlattices and multiple-quantum-well structures. Due to the breakdown of the lattice periodicity, optical phonons at points other than zone centre become observable in the Raman spectra as side bands on the low-frequency side of the LO phonon line [30, 31]. Similarly, confinement of optical phonons within a spherical particle also leads to considerable changes in the LO phonon line shape. The relaxation of the $k = 0$ selection rule results in a line shape given as [32, 33]

$$I(\omega) = \int \frac{|C(0,k)|^2}{[\omega - \omega(k)]^2 + (\Gamma_0/2)^2}\, \mathrm{d}^3k \qquad (2)$$

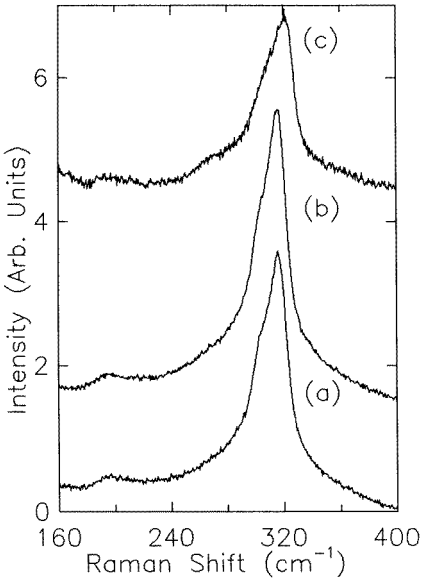

Figure 4. Raman spectra of the sample in the region of LO phonons. (a) The untreated sample, and the sample after annealing at (b) 500 °C and (c) 700 °C. Note the increase of the LO phonon frequency upon annealing. Spectrum (c) is magnified by a factor of ten for the sake of clarity.

where $\omega(k)$ is the phonon dispersion curve, Γ_0 is the natural full linewidth and $C(0,k)$ is the Fourier coefficient of the phonon confinement function which is often taken as a Gaussian [32]:

$$|C(k)|^2 = \exp(-k^2d^2/16\pi^2). \tag{3}$$

This line shape leads to marked asymmetry on the low-frequency side of the LO line and also a shift of the LO frequency to lower values. Figure 4 shows the Raman spectra of untreated GG475 and the annealed samples. Note the asymmetry of the LO phonon lineshape in all of the spectra. A weak peak is also observed at around 196 cm^{-1}. This corresponds to a CdSe-like mode arising from the two-mode behaviour of the $CdS_{1-x}Se_x$ mixed-crystal system. The positions of CdSe- and CdS-like modes have been reported over the complete composition range [34]. The position observed in the present study is consistent with the content of Se (5%) in the glass. Another important feature of these spectra is the position of the CdS-like LO mode. In the untreated samples it appears at 315 cm^{-1} while in pure CdS the LO phonon is observed at 303 cm^{-1}, and in the mixed crystal $CdS_{0.95}Se_{0.05}$ it is expected to be slightly lower. It may be mentioned that the mixed-crystal system $Zn_yCd_{1-y}S$ exhibits a one-mode behaviour and the LO phonon frequency varies from 303 cm^{-1} to 352 cm^{-1} as the composition y is varied from 0 to 1. In addition to the effects arising from compositional changes, an increase in the LO phonon frequency can occur due to strains. However, such a large increase of 12 cm^{-1} cannot be accounted for by strains alone. Furthermore, if strains were the cause of this increase the frequency would be expected to decrease upon annealing as the strains are removed due to heat treatment. In contrast, it is observed to increase by 5 cm^{-1} as compared to that for the untreated sample. Hence we ascribe this behaviour to the incorporation of Zn into the particle, and the composition may be expressed as $Zn_yCd_{1-y}S_{0.95}Se_{0.05}$. From the known compositional dependence of the phonon frequency in this mixed-crystal system [35], the Zn content y in

the particle is estimated to be 15.6% for the untreated sample and 22.7% after annealing at 600 °C for 5 h. The increase in the LO phonon frequency of CdS-doped Zn-containing glass reported recently [25] is similar to that found in the present studies. Annealing at still higher temperatures up to 700 °C does not cause further changes in the LO phonon frequency.

It may be mentioned that the untreated samples exhibit excellent resonance enhancement of the LO intensities with the 457.9 nm line of an argon-ion laser. However, this resonance enhancement disappears upon annealing. This is probably due to a shifting of the direct interband transition away from the laser line, resulting from the changes in particle composition and size. This is discussed in detail in a later section along with the overtone spectra.

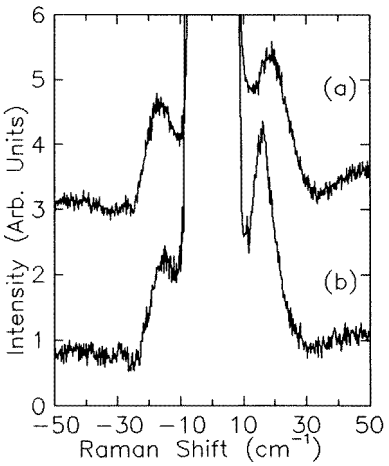

Figure 5. Stokes and anti-Stokes low-frequency polarized (VV) Raman spectra of semiconductor nanoparticles obtained using the 501.7 nm line of an argon-ion laser, before (a) and after (b) annealing at 600 °C. The peaks arise due to the spheroidal mode of the particle.

3.3. Low-frequency Raman scattering

Confinement of acoustic phonons within the particles also leads to the appearance of new modes in the vibrational spectrum of the material. These modes correspond to the spheroidal and torsional vibrations of the sphere; the former is associated with dilatation while this is not the case with the latter. According to Lamb's theory, the spheroidal mode frequencies depend on the material properties through the longitudinal and transverse sound velocities (v_l and v_t) while the torsional modes do not [36, 37]. Furthermore, the frequencies of these modes depend inversely upon the diameter of the particle and lie within the range of a few cm^{-1} to a few tens of cm^{-1}. These modes are characterized by two indices l and n, where l is the angular momentum quantum number and n is the branch number [12]. From group theoretical considerations it has been shown that only even-l spheroidal modes can be Raman active while torsional modes are Raman inactive [38]. For CdS particles, the frequency of the $l = 0$ and $n = 2$ spheroidal mode at $v_l/v_t = 2.3$ is given as [29]

$$\omega = 0.9\frac{v_l}{dc} \tag{4}$$

where d is the diameter of the particle and c is the velocity of light. This value of v_l/v_t is nearly the same for CdSe also and hence the above equation remains valid for $CdS_{1-x}Se_x$ particles. It may further be pointed out that the spheroidal mode ($l = 0$) is observed only in the polarized configuration whereas the quadrupolar modes ($l = 2$) can be detected in polarized as well as depolarized geometries [29]. Hence, polarized measurements in the low-frequency region are useful in unambiguous identification of spheroidal modes.

In order to measure the frequencies of the spheroidal modes of the particles, low-frequency Stokes and anti-Stokes spectra of untreated samples and those of annealed samples at various temperatures between 500 and 700 °C are recorded covering a range from −100 to 100 cm^{-1}. Both Stokes and anti-Stokes spectra are recorded in a single scan; close to the Rayleigh line the intensity is reduced using appropriate filters. Figure 5 shows the polarized LFR spectra of samples before and after annealing at 600 °C for 5 h. In the depolarized geometry no clear modes were detected, suggesting that the surface modes do not have sufficient intensity in the present case. In the untreated samples the spheroidal mode appears at 17.5 cm^{-1}. Substituting a value of 3813 m s^{-1} for the longitudinal sound velocity, appropriate for $Zn_{0.16}Cd_{0.84}S_{0.95}Se_{0.05}$ in equation (4), the particle size is estimated to be 6.5 nm in the untreated sample. This value is close to that communicated by the supplier [28] whereas after annealing it shifts to lower frequencies and a decrease in the spheroidal mode frequency suggests an increase in the particle size subsequent to annealing. The longitudinal sound velocities used for the calculation of the particle size after different annealing treatments are corrected for the true Zn concentration in the particle, which is estimated from the 1-LO Raman frequencies.

Figure 6 shows the variation of the spheroidal mode frequency and the estimated particle diameter as a function of annealing temperature. Note that significant growth of the particles takes place only above 550 °C. This is consistent with the observations reported by other investigators [25, 39]. Annealing at 625 °C for five hours leads to a particle size of 8.7 nm. However, for annealing above 625 °C, identification of the spheroidal mode becomes difficult. Now a few remarks about the wavelength dependences of spheroidal mode spectra are in order. LFR spectra are recorded using several wavelengths of argon- and krypton-ion lasers in the range 406.7 to 514.5 nm. It is found that when the exciting radiation is in close proximity to the electronic interband transition in the particle, the spheroidal modes are not easily detected, whereas these are seen much more clearly when the photon energy is away from resonance. For example, wavelengths of 476.2 nm and longer are found to give excellent LFR signals (the intensity of the LFR spectrum excited with 501.7 nm is maximal) whereas the 465.8 nm and shorter lines yield much weaker spectra. This is understandable because when exciting radiation is in resonance with the electronic interband transition, the low-frequency spectrum is always accompanied by a large luminescence background, making detection of spheroidal modes difficult. On the other hand, resonance enhancements of spheroidal and surface modes have been reported for excitation wavelengths close to that of excitonic absorption [29]. The present observation is consistent with a recent report of LFR spectrum of GG495 obtained using the 514.5 nm line being more intense than that obtained using the 488 nm line [39]. However, the authors of [39] attribute their observations to resonance enhancement, even though the 514.5 nm line is far away from the electronic transition (the band gap) in GG495.

3.4. The origin of the blue-shift

The particle diameter and its composition having been estimated, the blue-shift of the PL energy as a function of the annealing temperature can now be understood as follows. As

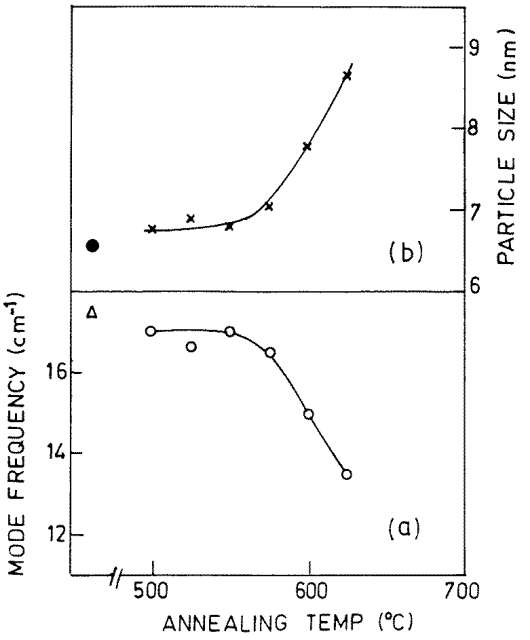

Figure 6. (a) The dependence of the spheroidal mode frequency on the annealing temperature. The symbol △ represents the frequency corresponding to the untreated sample. (b) The estimated particle size as a function of the annealing temperature. The sound velocities used in the calculations correspond to the actual composition of the particles (see the text). The symbol ● corresponds to the size in the untreated sample.

discussed in the previous section, in addition to the growth in particle size, a change in composition also takes place. The bulk band gap of $Zn_yCd_{1-y}S$ mixed crystals is known to increase with the concentration of Zn [25]. Hence one can understand this blue-shift of the PL energy if the increase in the bulk band gap more than compensates the red-shift arising from the particle size growth. Although the behaviours of the optical properties of Zn-containing semiconductor-doped glass [20, 26] are reported to be different from those for glass without Zn [24, 27], a blue-shift of the PL energy observed in the present investigations has not been reported earlier. It is important to compare the effects of the annealing on the composition, the particle size and the PL energy. Significant particle size growth takes place only above 575 °C whereas the PL energy continuously increases in this temperature range. This suggests that most of the blue-shift of the PL energy arises due to compositional changes. On the other hand, during annealing at $T \geqslant 600$ °C, the particle composition does not increase beyond 22.7%, while the particle size increases substantially. Hence a marginal decrease (red-shift) of the PL energy above 600 °C probably arises from the particle growth.

The difference between the present results and those reported in [25] can be understood in the following way. The annealing studies of Yukselici *et al* [25] represent the 'early stage' of nucleation and growth where the particle sizes are small. Furthermore, during this stage the composition of Zn in the particle is also small as is evident from the evolution of the LO phonon frequency during annealing. In view of the small size of the particle and the low values of y, the quantum confinement effects dominate over the compositional changes resulting in a red-shift of the optical absorption. The untreated samples used in the present study (filter GG475) have actually undergone heat treatments at Schott Glaswerke resulting

in substantial growth of the particle size and increase in Zn content in the particles. The present annealing treatments of these samples show that while the particle size continues to increase, the composition y also increases substantially. However, in this regime the effect of a change in y on the optical properties dominates over that due to the particle size growth. Consequently, a blue-shift is observed. Thus the present annealing studies represent the 'late stage' of particle growth and are complementary to the previous studies on the 'early stages' of nucleation and growth [25]. It may be pointed out that in CdSe-doped glasses, Zn is not found to enter the particles [20], in contrast to the behaviour of CdS-doped glass. The difference between the two behaviours has been attributed to the departure of the stoichiometry from that of the ideal II–VI compound semiconductor.

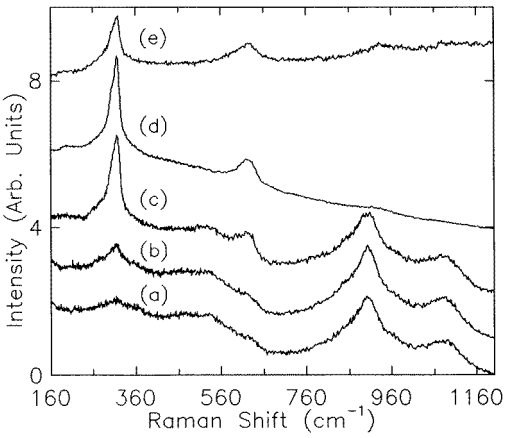

Figure 7. Raman spectra of untreated semiconductor nanoparticles excited using several wavelengths, (a) 514.5, (b) 496.5, (c) 476.5, (d) 457.9 and (e) 406.7 nm, of argon- and krypton-ion lasers, exhibiting resonance enhancement at 457.9 nm. The spectra (a), (b), (c) and (e) are magnified by factors of 18, 14, 9 and 12 respectively.

3.5. Resonance effects on LO phonons and their overtones

As mentioned earlier, LO phonons exhibit excellent resonance enhancement of the Raman intensities in the untreated samples with the 457.9 nm line of an argon-ion laser. In order to examine the wavelength dependence of the intensities of LO phonons and their overtones, Raman spectra are recorded for several wavelengths in the region of 406.7 and 514.5 nm. Figure 7 shows the Raman spectra over an extended range of Raman shifts up to 1200 cm^{-1}. Note that the intensity of the LO phonon is maximal for the 457.9 nm line and it decreases when the exciting photon energy is either decreased or increased. This is understandable, as the photon energy corresponding to 457.9 nm (2.708 eV) is rather close to the PL energy (2.678 eV) of the untreated sample. Hence the condition for an *out*-resonance is nearly satisfied.

One can also notice in figure 7 the presence of overtones of LO phonons in the Raman spectra. A peak at 625 cm^{-1} can be assigned to 2-LO phonons. There also appears a weak peak in the 3-LO region at around 910 cm^{-1} superimposed on a large luminescence background. It may be mentioned that the region of Raman shifts in the range 800 to 1200 cm^{-1} also has vibrational modes intrinsic to base glass arising from its molecular-like units. In order to confirm the presence of 3-LO phonons, the Raman spectrum of GG475 is

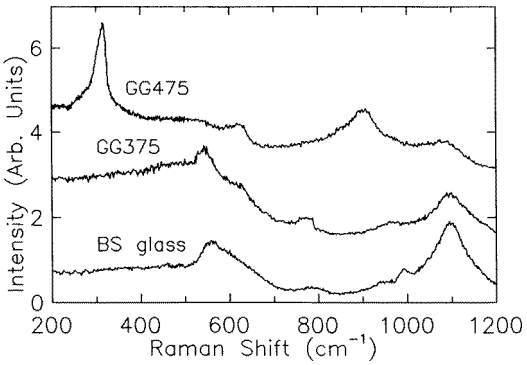

Figure 8. Comparison of the Raman spectrum of semiconductor nanoparticles (GG475) (excitation λ: 457.9 nm) with those of an ionically coloured glass (GG375) (excitation λ: 476.2 nm) and a borosilicate glass window (excitation λ: 457.9 nm). Note the absence of a 3-LO peak at around 910 cm^{-1} in the glasses not containing semiconductor particles. The peak at 1075 cm $^{-1}$ arises due to glass host.

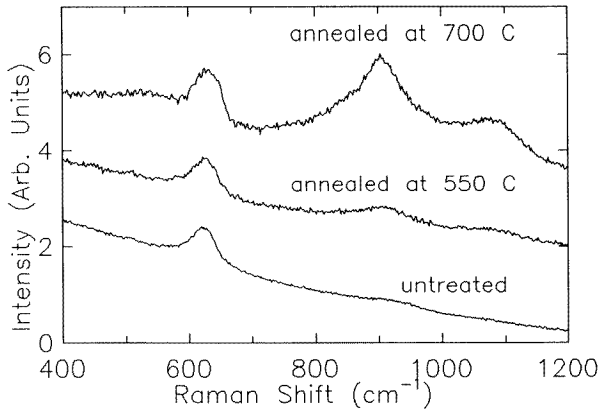

Figure 9. Raman spectra of the overtones of LO phonons (excitation λ: 457.9 nm) for untreated semiconductor nanoparticles and after annealing at 550 and 700 °C. The spectra at 550 and 700 °C are magnified by factors of 5 and 14 respectively for the sake of clarity.

compared with those of an ionically coloured glass (GG375) and an undoped borosilicate glass in figure 8. Note that the peak at 910 cm^{-1}, present for GG475, is absent for other glasses. In view of this, this peak can be assigned to 3-LO phonons. Upon annealing, the intensity of 2-LO phonons is also found to decrease, similarly to the case for 1-LO phonons. Figure 9 shows the overtone spectra of samples annealed at several temperatures. Note that the decrease of the photoluminescence intensity makes 3-LO phonon and other modes of the glass host emerge clearly out of the background. The decrease of the intensity of the overtones occurs because of the energy of the direct interband transition (band gap) moving away from the exciting photon energy.

At first, it may appear that the evolution of the present system of nanoparticles from $CdS_{0.95}Se_{0.05}$ (ternary) to $Zn_yCd_{1-y}S_{0.95}Se_{0.05}$ (quaternary) makes the system more complex, and a study of a system with fewer constituents will probably be easily interpretable. In this context it may be mentioned that since Se constitutes only 5% of the sample, its effect on the

properties is only marginal and one can still consider the present system as a pseudo-ternary $Zn_yCd_{1-y}S$ system. Furthermore, the motivation of the present investigations has been that of studying the influence of Zn on the 'late stage' of the annealing of semiconductor-doped glass. From this point of view the results obtained in the present study provide further information on their annealing behaviour.

From the analysis of the present results in the light of those reported earlier [25, 29] the following complete understanding of the annealing behaviour emerges. The blue-shift of the optical absorption with respect to that of bulk semiconductor first decreases and then it increases. The decrease of the blue-shift during the 'early stage' of the annealing arises primarily from the decrease of the quantum confinement energy as the particle grows. During this stage, the incorporation of Zn in the particles is insignificant. The increase in the blue-shift found in the 'late stage' of the annealing arises mainly from the incorporation of Zn into the particles, and the contribution of the quantum confinement energy to the optical properties is rather small during this stage.

4. Summary and conclusions

Optical and vibrational properties of semiconductor nanoparticles dispersed in an oxide glass host are investigated as a function of the annealing temperature. LO phonon and spheroidal mode frequencies are used to estimate the composition and size of the particles. The present annealing treatments represent the 'late' stage of particle growth. The blue-shifts of the optical absorption and photoluminescence occurring as a result of the annealing arise from the change in the stoichiometry of the particle, which more than compensates the red-shift arising from the particle growth. The accompanying changes in the LO phonon spectra are also consistent with the composition of the particle. The resonance enhancements of the LO phonon and its overtones with the 457.9 nm line of an argon-ion laser are found to arise due to direct interband (band-gap) transition in the particle.

Acknowledgments

The authors acknowledge the help of Mr G V N Rao in the XRD measurements, Head/Water and Steam Chemistry Laboratory for permitting the use of the UV-VIS Spectrophotometer and Mrs Padmakumari and Mr Rajaraman for help in the absorption measurements. It is a pleasure to thank Mr K D Loosen of Schott Glasswerke for supplying the typical compositional data for filter glasses. We also thank Dr T S Radhakrishnan for his keen interest in the work and Dr Baldev Raj and Dr P Rodriguez for their encouragement.

References

[1] Warnock J and Awschalom D D 1985 *Phys. Rev.* B **32** 5529
[2] Eychmuller A, Katsikas L and Weller H 1990 *Langmuir* **6** 1605
[3] Brus L E 1984 *J. Chem. Phys.* **80** 4403
[4] Nair S V, Sinha S and Rustagi K C 1987 *Phys. Rev.* B **35** 4098
[5] Rustagi K C and Bhawalkar D D 1990 *Ferroelectrics* **102** 367
[6] Remitz K E, Neuroth N and Spert B 1991 *Mater. Sci. Eng.* B **9** 413
[7] Bret G and Gires F 1964 *Appl. Phys. Lett.* **4** 175
[8] McCall S L and Gibbs H M 1978 *J. Opt. Soc. Am.* **68** 1378
[9] Maeda Y, Tsukamoto N, Yazawa Y, Kanemitsu Y and Masumoto Y 1991 *Appl. Phys. Lett.* **59** 3168
[10] Takagahara T and Takeda K 1992 *Phys. Rev.* B **46** 15 578
[11] Rodden W S O, Torres C M S and Ironside C N 1995 *Semicond. Sci. Technol.* **10** 807

[12] Tanaka A, Onari S and Arai T 1993 *Phys. Rev.* B **47** 1237
[13] Champagnon B, Andrianasolo B, Ramos A, Gandais M, Allais M and Benoit J P 1993 *J. Appl. Phys.* **73** 2775
[14] Tanaka A, Onari S and Arai T 1992 *Phys. Rev.* B **45** 6587
[15] Efros Al L, Ekimov A I, Kozlowski F, Petrova-Koch V, Schmidbaur H and Shumilov S 1991 *Solid State Commun.* **78** 853
[16] Chestnoy N, Hull R and Brus L E 1986 *J. Chem. Phys.* **85** 2237
[17] Herron N, Wang Y and Eckert H 1990 *J. Am. Chem. Soc.* **112** 1322
[18] Mei G 1992 *J. Phys.: Condens. Matter* **4** 7521
[19] Sekikawa T, Yao H, Hayashi T and Kobayashi T 1992 *Solid State Commun.* **83** 969
[20] Borrelli N F, Hall D W, Holland H J and Smith D W 1987 *J. Appl. Phys.* **61** 5399
[21] Banfi G, Degiorgio V, Rennie A R and Barker J G 1992 *Phys. Rev. Lett.* **69** 3401
[22] Liu L C and Risbud S H 1990 *J. Appl. Phys.* **68** 1218
[23] Fuyu Y and Parker J M 1988 *Mater. Lett.* **6** 233
[24] Ekimov A I, Efros Al L and Onushchenko A A 1985 *Solid State Commun.* **56** 921
[25] Yukselici H, Persans P D and Hayes T M 1995 *Phys. Rev.* B **52** 11 763
[26] Sukumar V and Doremus R H 1993 *Phys. Status Solidi* b **179** 307
[27] Potter B G Jr and Simmons J H 1988 *Phys. Rev.* B **37** 10 838
[28] Loosen K D 1996 private communication
[29] Champagnon B, Andrianasolo B, and Duval E 1991 *J. Chem. Phys.* **94** 5237
[30] Sood A K, Manendez J, Cardona M and Ploog K 1985 *Phys. Rev. Lett.* **54** 2111
[31] Arora A K, Suh E K, Ramdas A K, Chambers F A and Moretti A L 1987 *Phys. Rev.* B **36** 6142
[32] Campbell I H and Fauchet P M 1986 *Solid State Commun.* **58** 739
[33] Tiong K K, Amirtharaj P M, Pollak F H and Aspnes D E 1984 *Appl. Phys. Lett.* **44** 122
[34] Tu A and Persans P D, 1991 *Appl. Phys. Lett.* **58** 1506
[35] Vodop'yanov L K, Umarov B S, Sysoev L A and Sarkisov L A 1971 *Pis. Zh. Eksp. Teor. Fiz.* **13** 507 (Engl. Transl. 1971 *JETP Lett.* **13** 660)
[36] Lamb H 1982 *Proc. Lond. Math. Soc.* **13** 189
[37] Tamura A, Higeta K and Ichinokawa T 1982 *J. Phys. C: Solid State Phys.* **15** 4975
[38] Duval E 1992 *Phys. Rev.* B **46** 5795
[39] Roy A and Sood A K 1996 *Solid State Commun.* **97** 97